Background for Machine Learning

Recent advancements in machine learning models have led to significant improvement in the performance of fields such as image processing, natural language processing and a plethora of time series classification and generation tasks in biomedical research. Broadly, machine learning techniques can be divided into supervised and unsupervised algorithms. Supervised algorithms are trained on labelled data using the difference between the predicted and actual output for optimizing the model. After sufficient training, the model can successfully predict labels (values) for new inputs. Unsupervised algorithms, on the other hand, analyzes a given set of unlabeled (in the context of this study, unscored) data and draws inferences without using any label information. Mostly, unsupervised algorithms are used for exploratory analysis to find hidden patterns in a dataset.

Deep Neural networks (DNNs), a type of machine learning model, comprises multiple layers of a collection of connected units called *artificial neurons*. An artificial neuron receives a set of input signals and transmits the activated output to its subsequent connected neurons using non-linear activation functions. DNNs have advanced state-of-the-art performance across different domains. Broadly, two types of neural networks are used: (1) Convolutional Neural Network (CNN) and (2) Recurrent Neural Networks (RNN). The convolution in CNN indicates that the network employs the mathematical operation called *convolution*. CNNs are neural networks that use convolution in place of general matrix multiplication in its respective layers. CNN's have proven to be useful in various image processing and computer vision tasks for e.g., image deblurring, image classification, and image segmentation. RNNs, on the other hand, exhibit temporal behavior due to directed connections between units of an individual layer and have achieved significant results in tasks such as machine translation, text-to-speech synthesis, and sentiment analysis. They allow previous outputs to be used as inputs while having hidden states. Hidden states, basically, transfer input representation of the previous timestamps to the

current timestamp. Hochreiter et al. [1] and Bengio et al. [2] found that RNNs were not able to learn long-term dependencies in temporal signals and often looked at just the recent information for completing tasks. Long-Short Term Memory networks (LSTM) [3] are a special kind of RNNs that are capable of learning long-term dependencies. They were designed to solve two inherent problems encountered in RNNs: (1) remembering information for long periods of time, and (2) the vanishing gradient problem while training RNNs. Structurally, they are similar to RNNs, but they have a *cell* unit that remembers values over arbitrary time intervals.

Proposed Model

In our work, we used AutoEncoders (AEs), a type of DNNs, that explored the dataset to learn efficient data representation in an unsupervised manner. The primary function of the AE was to learn a latent representation (encoder) for a set of data in order to generate the original input (decoder) from the reduced encoded data representation. We developed a novel form of LSTM AutoEncoder that learned these latent representations from temporal polysomnography (PSG) data using LSTM layers. We trained two LSTM AutoEncoders for learning the latent representation of the seventeen PSG signals and the blood pressure signals and one LSTM AutoEncoder block (defined as mapper in Figure 1) for learning the function that projected a PSG data representation to its corresponding systolic and diastolic blood pressure representation. The decoder block of the blood pressure AE thus generated the corresponding blood pressure signal for a given set of PSG signals. As described before, the AE comprised of two main functions: (1) an encoder function $\boldsymbol{E}: \boldsymbol{X} \longrightarrow \boldsymbol{Z}$, that mapped an input signal $\boldsymbol{X}$ into a new vector space which in known as the latent space $\boldsymbol{Z}$, and (2) a decoder function $\boldsymbol{D}: \boldsymbol{Z} \longrightarrow \boldsymbol{X}$ which mapped the data from the latent space back to the original input space $\boldsymbol{X}$. Hence, the AE was defined as:

$$\widehat{\boldsymbol{X}}: \boldsymbol{D}(\boldsymbol{E}(\boldsymbol{X})) \qquad (1)$$

where, $\widehat{\boldsymbol{X}}$ was defined as the reconstructed signal.

$\boldsymbol{X_{PSG}}$ represented a given set of PSG signals. Hence, $\boldsymbol{X_{PSG}} \in \mathbb{R}^{30 \times 17}$ as we have seventeen different PSG signals, each taken at 30 seconds epoch, was our input. Similarly, $\boldsymbol{X_{BP}} \in \mathbb{R}^{30 \times 1}$ represented the corresponding systolic and diastolic blood pressure signals.Based on Equation. (1), we mathematically defined our proposed model using the following equations:

$$\widehat{\boldsymbol{X}}_{\boldsymbol{PSG}} = \boldsymbol{D_{PSG}}\left(\boldsymbol{E_{PSG}}\left(\boldsymbol{X_{PSG}}\right)\right), \quad (2)$$

$$\widehat{\boldsymbol{X}}_{\boldsymbol{BP}} = \boldsymbol{D_{BP}}\left(\boldsymbol{E_{BP}}\left(\boldsymbol{X_{BP}}\right)\right), \quad (3)$$

$$\widehat{\boldsymbol{X}}_{\boldsymbol{M}} = \boldsymbol{D_{BP}}\left(\boldsymbol{M}\left(\boldsymbol{E_{PSG}}\left(\boldsymbol{X_{PSG}}\right)\right)\right) \quad (4)$$

where, $\boldsymbol{D_{PSG}}$, $\boldsymbol{D_{BP}}$, $\boldsymbol{E_{PSG}}$, and $\boldsymbol{E_{BP}}$ were the decoder and encoder blocks for the PSG and BP AE models respectively. $\boldsymbol{M}$ denoted the mapper LSTM block that projected the PSG latent representation to its corresponding BP latent representation. We used $\boldsymbol{l_2}$ reconstruction loss function for training our individual LSTM-AE and the mapper blocks. For every iteration, the three models were optimized in an end-to-end manner. The loss functions were defined as follows:

$$\boldsymbol{L_{PSG}} = \left\|\widehat{\boldsymbol{X}}_{\boldsymbol{PSG}} - \boldsymbol{X_{PSG}}\right\|, \quad (5)$$

$$\boldsymbol{L_{BP}} = \left\|\widehat{\boldsymbol{X}}_{\boldsymbol{BP}} - \boldsymbol{X_{BP}}\right\|, \quad (6)$$

$$\boldsymbol{L_{M}} = \left\|\widehat{\boldsymbol{X}}_{\boldsymbol{M}} - \boldsymbol{X_{BP}}\right\|, \quad (7)$$

The model was trained for 2000 iterations using RMSprop optimizer.

References

[1] Hochreiter, Sepp. "Untersuchungen zu dynamischen neuronalen Netzen." Diploma, Technische Universität München 91, no. 1 (1991).

[2] Bengio, Yoshua, Patrice Simard, and Paolo Frasconi. "Learning long-term dependencies with gradient descent is difficult." IEEE transactions on neural networks 5, no. 2 (1994): 157-166.

[3] Hochreiter, Sepp, and Jürgen Schmidhuber. "Long short-term memory." Neural computation 9, no. 8 (1997): 1735-1780.

Figures

Figure S1. Correlation plots for Blood Pressure predictions with their respective degrees of freedom (DOF):

A. Continuous Blood Pressure prediction

Baseline: (DOF=77896)

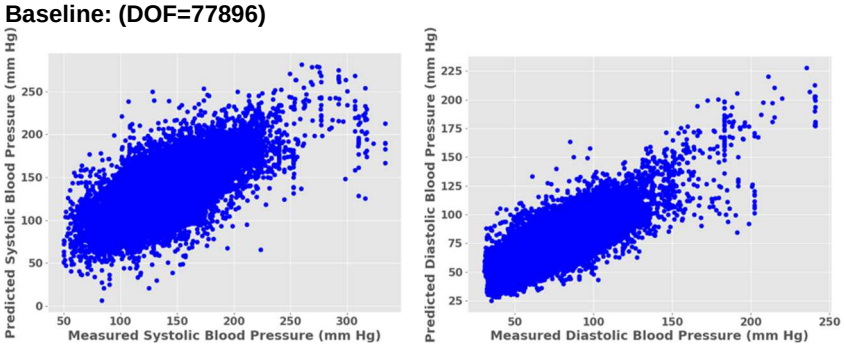

Titration: (DOF=181731)

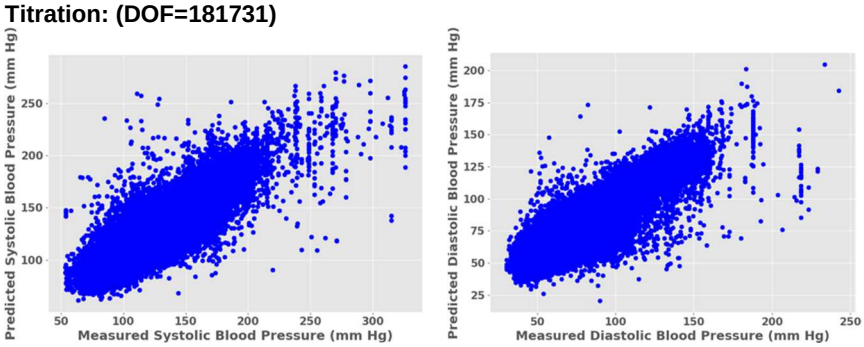

B. Post-respiratory event surge in Blood Pressure

Baseline: (DOF=86578)

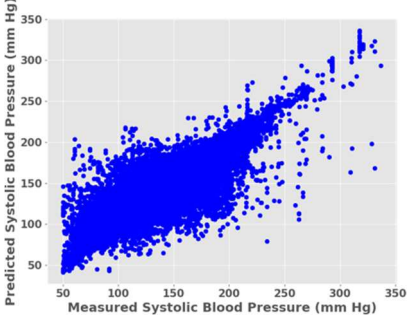

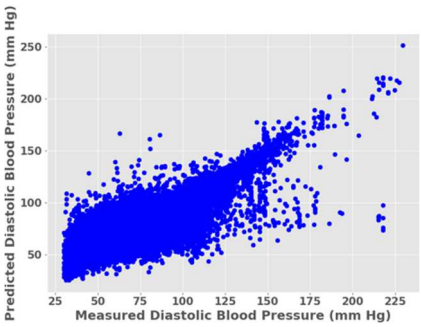

Titration: (DOF=51868)

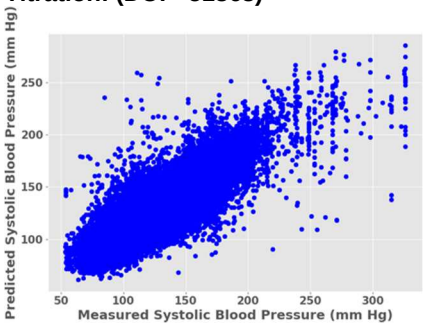

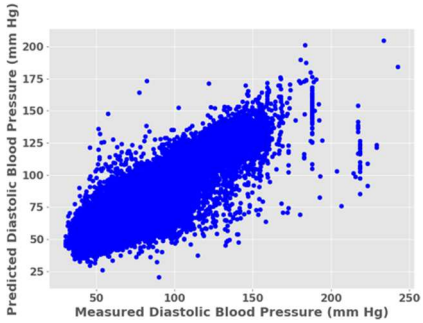

Baseline + Titration: (DOF=138058)

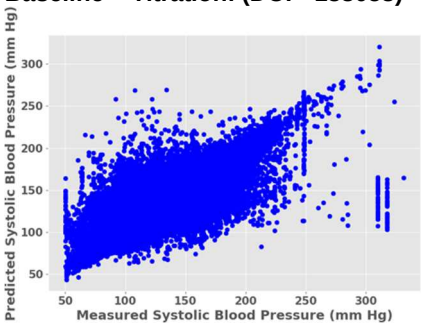

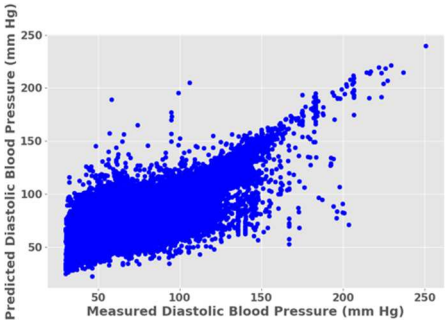

Figure S2. Data distribution plots of measured and predicted Blood Pressure

A. Continuous blood pressure prediction

Baseline:

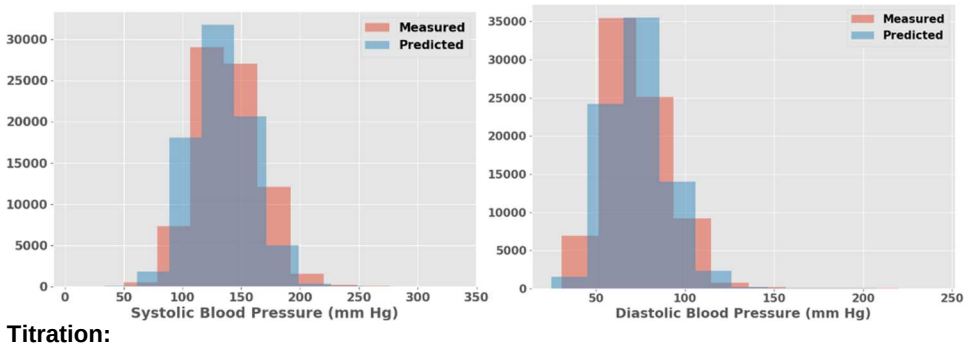

Titration:

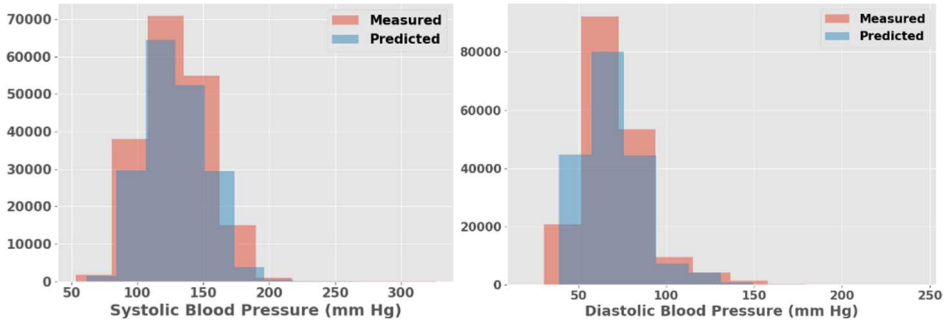

B. Post-respiratory event surge in Blood Pressure

Baseline:

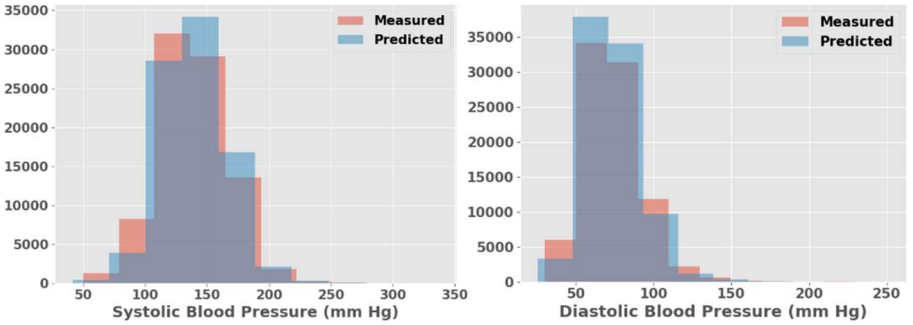

Titration:

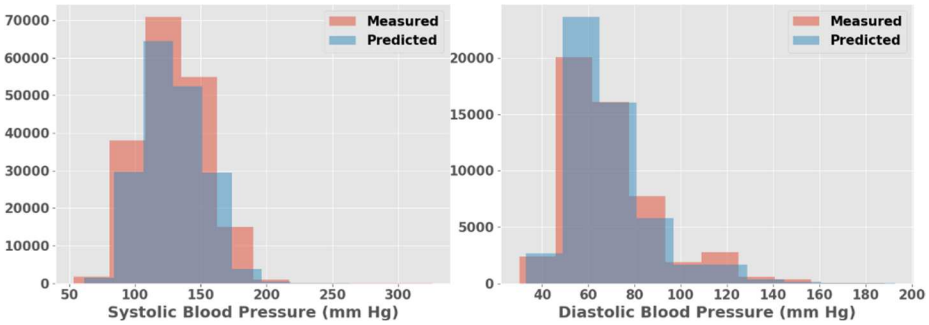

Baseline + Titration:

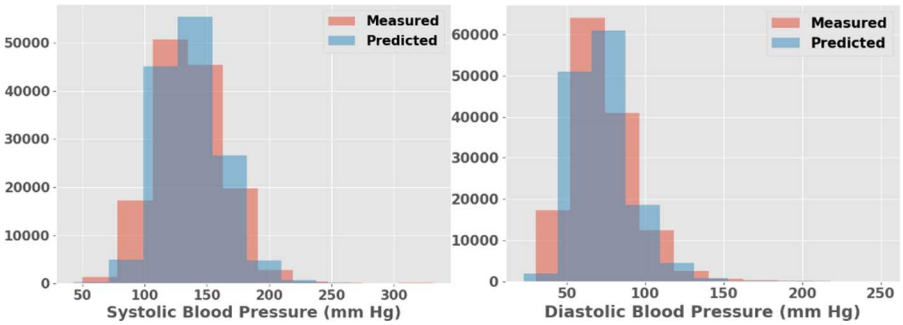

Importance of Different Polysomnography Signals in Blood Pressure Prediction

We explored the contribution of various polysomnography signals in the DNN model for post-apnea blood pressure prediction with ablation analyses. Briefly, each signal was removed, one at a time, from the full model (of input signals) to assess the change in correlation. The signal removal that was associated with significant reduction in correlation (to ≤0.15) as compared to the full model (≥0.75) may be considered important or necessary for blood pressure prediction. These correlations are highlighted in bold in Table S1. Overall, the EEG and respiratory signals appeared to have important contributions to post-respiratory event blood pressure prediction. Although exploratory, these results provide some biological plausibility to the proposed model. We believe a similar approach can be taken in future studies to determine the necessary polysomnography signals for accurate blood pressure prediction.

Table S1. Ablation analyses for post-respiratory event surge in Blood Pressure

Dataset	Baseline		Titration		Baseline + Titration	
	DBP	SBP	DBP	SBP	DBP	SBP
F3-M2	0.39±0.07	0.51±0.03	0.29±0.10	**0.08±0.04**	0.32±0.05	0.32±0.04
C3-M2	0.31±0.05	0.41±0.03	0.29±0.12	0.32±0.13	0.31±0.03	0.33±0.07
O1-M2	0.16±0.05	**0.12±0.06**	0.43±0.09	0.25±0.10	0.17±0.06	**0.07±0.04**
F4-M1	0.17±0.05	0.21±0.05	0.40±0.02	0.13±0.05	0.17±0.03	0.22±0.08
C4-M1	0.35±0.05	0.45±0.02	0.38±0.12	**0.11±0.08**	0.32±0.05	0.30±0.02
O2-M1	0.10±0.08	**0.08±0.05**	0.32±0.13	0.21±0.06	0.27±0.09	**0.12±0.01**
LOC	0.14±0.06	0.19±0.04	**0.007±0.06**	0.13±0.09	**0.07±0.04**	0.17±0.04
ROC	**0.076±0.03**	0.16±0.02	**0.007±0.07**	0.13±0.07	**0.10±0.02**	**0.10±0.05**
CHIN	0.67±0.04	0.79±0.02	0.55±0.06	0.45±0.13	0.70±0.02	0.62±0.18
LEGS	0.60±0.04	0.70±0.02	0.47±0.04	0.38±0.07	0.54±0.06	0.65±0.03
SNORE	0.68±0.03	0.81±0.02	0.37±0.11	0.37±0.10	0.67±0.02	0.66±0.02
TcCO2	0.29±0.02	0.20±0.01	0.34±0.02	0.24±0.03	0.23±0.02	0.27±0.02
NPT	**0.08±0.06**	**0.05±0.04**	0.17±0.06	**0.04±0.05**	**0.01±0.05**	**0.07±0.05**
THERM	**0.07±0.04**	**0.05±0.05**	0.53±0.13	0.41±0.09	**0.07±0.07**	**0.05±0.08**
CHEST	0.13±0.02	0.17±0.01	**0.13±0.07**	**0.11±0.10**	0.12±0.03	0.19±0.04
ABDMN	**0.05±0.08**	**0.07±0.02**	**0.00±0.09**	0.13±0.06	**0.06±0.02**	0.14±0.03
SAO2	**0.03±0.03**	0.13±0.07	**0.15±0.02**	**0.03±0.03**	0.14±0.02	0.13±0.05

Key: The first six signals are electroencephalography named per standard nomenclature, LOC and ROC are eye movement signals, Chin is chin electromyography (EMG), Legs is lower extremity EMG (right and left combined), TcCO2 is transcutaneous CO2, NPT is nasal pressure transducer, THERM is nasal thermistor, CHEST and ADBMN are effort signals and SaO2 is pulse oximetry.